

STRUCTURE OF OPTIMAL CONTROL IN OPTIMAL SHAPING OF THE STEEL ARCH

Leszek MIKULSKI, Dorota JASIŃSKA*, Olga DĄBROWSKA
Cracow University of Technology

Abstract

The paper presents the problem of optimal shaping of the H-bar cross-section of a steel arch that ensures minimal mass. Nineteen combinations of nine basic load states are considered simultaneously in the problem formulation. The optimal shaping task is formulated as a control theory problem within the formal structure of the maximum Pontriagin's principle. Since the ranges of constraint activity defining the control structure are a priori unknown and must be determined numerically, assuming the proper control structure plays a key role in the task solution. The main achievement of the present work is the determination of a solution of the multi-decision and multi-constraint optimization problem of the arch constituting a primary structural system of the existing building assuring the reduction of the structure mass up to 42%. In addition, the impact of the assumed state constraint value on the solution structure is examined.

Keywords: shape optimization, optimal control, arch, multipoint boundary value problem

1. INTRODUCTION

Arches have been used in engineering practice for millennia and are still widely applied to large-span roof structures. Despite the rich research literature, there are still challenges in arch shape optimization. If properly shaped, arches are efficient structures that transmit loads to foundations [31] while having relatively low self-

*Corresponding author: Dorota Jasińska: Faculty of Civil Engineering, Cracow University of Technology, Warszawska 24, 31-155 Cracow, Poland, dorota.jasinska@pk.edu.pl

weight. The load-carrying efficiency is the result of the domination of axial loads with small eccentricity [1, 16, 30]. Additional material savings can be obtained by optimizing the shape of the arch while taking into account imposed constraints [4, 10, 11, 12]. Optimal shaping of moment-free arches under the action of self-weight and constant distributed loads can be found in [13]. The finite element method is used in [28] to minimize the volume of the arch with variable cross-sectional dimensions. The analytical design criteria for the optimal shape of statically determinate arches with vertical loads in key sections under the assumption of constant normal stress are presented in [15] and [24]. Oftentimes the key issue is the minimization of the arch volume, since self-weight is the dominating vertical load, comprising about half of the total loading. Some recent works touch on the topic of optimal design of arches with minimal volume, while considering different constraints imposed on the end segments, using semi-analytical methods [25, 26, 27], or optimal control [6]. Engineering structures, depending on their intended use, must meet a number of criteria, often going beyond safety measures. Solutions should be economical in terms of material use and labor costs. In optimization practice, deliberations are often limited to easily defined structural aspects, e.g., the most favorable cross-section shape, the axis curvature, or location of supports. Among many factors that affect the structure performance, the reduction of material consumption plays a key role. Minimizing the self-weight of the structure, while maintaining its function and satisfying the safety criteria, can positively impact the total cost of a project, especially for large structures.

The formulation of optimization problems requires the creation of a mathematical model and the definition of state variables, control, constraint conditions, and an objective function. The Pontriagin's maximum principle allows for the formulation of a set of necessary optimality conditions in the form of a multipoint boundary value problem for a set of ordinary differential equations or, more generally, a differential-algebraic boundary value problem [17, 18]. The most important steps in proper problem formulation are: choice of the objective function, decision variables, and necessary constraints, which can depend on state variables and decision variables [21,22]. The issues regarding the necessary optimality conditions for control problems with pure state constraints are still an ongoing topic of research [7, 9, 14].

The tasks of optimal shaping of realistic civil engineering structures are characterized by multiple controls and constraints, as well as taking into account numerous load states, which results in a large number of state equations. In these cases, special attention must be paid to the control structure, i.e. to the appropriate sequence of controls obtained from different conditions. Despite a reach literature published in recent years on the development of arch-shaped optimization [2, 8, 20, 23, 25], to the best authors' knowledge these works do not include research in

the area of optimal control. The present work is a continuation of the research topic presented in [6]. The subject of the multi decision optimization is the arch constituting a primary structural system of the existing building (old opera house in Cracow, Poland), under actions of multiple load combinations and with several constraints imposed by appropriate design standards. Since the work focuses on the task of shape optimization, second-order effects such as material and geometrical nonlinearities, stability issues, or spatial structure work are disregarded in the considerations. The objective is to determine the variable cross-section dimensions of an H-bar arch girder, under the action of self-weight and multiple external loads, ensuring minimal volume, as well as the fulfillment of standard requirements (load bearing capacity and deflection limit). The task is formulated as a non-autonomous control theory problem within the formal structure of Pontriagin's maximum principle with state and state-control constraints. The multipoint problem obtained from Hamiltonian minimization is solved numerically by the Dircol-2.1 software [29] using the direct collocation method, and the optimal cross-sections are obtained together with graphs of internal forces and deflections. The chosen theoretical foundations of the above-mentioned methods are presented in [19, 21].

The optimal solutions obtained by control theory methods for different assumed admissible arch deflections are independently verified by finite element method (FEM) computations.

The article is organized as follows. Sect. 2 starts with the description of the optimized structure and load states taken into account, followed by the list of state equations and assumed constraints and restrictions. Then, in Sect. 3 the optimization task is formulated within the formal structure of the Pontriagin's maximum principle. The necessary optimality conditions for the non-autonomous problem with state-control as well as pure state constraints are discussed in detail. In Sect. 4 the obtained optimal solutions are presented, and the dependence of the control structure on the state constraint is discussed and the benefits resulting from optimization are analyzed. Additionally, the fulfillment of serviceability and ultimate limit states by obtained optimal arch girders is verified by FEM computations. Section 5 concludes the article with a brief summary.

2. DESCRIPTION OF OPTIMIZED STRUCTURE AND TECHNICAL ASSUMPTIONS

The optimized arch constitutes the roof girder of a hall of horizontal dimensions 21 by 50 m, with girder spacing equal to 2.5 m. The arch is 20.754 m long, 4.255 m high (see Fig. 1a), with the parabolic axis and the H-bar cross-section. The following cross-sectional dimensions are constant: the web height and flange

thickness (see Fig. 1b), whereas the web thickness (U_1) and flange width (U_2) are the subjects of optimization.

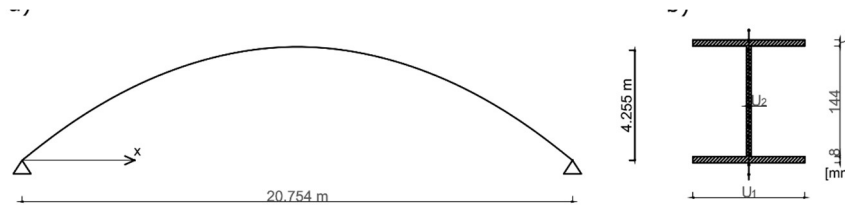


Fig. 1. Arch diagram (a) and cross-section (b)

2.1. Acting loads

To take into account all possible load combinations, 9 basic load states are defined according to applicable standards [3] (Fig. 2, Table 1). Due to the large number of possible combinations of the basic loads listed above, in order to reduce the dimension of the optimization problem, the task is formulated in one characteristic interval. Such a formulation is possible when only distributed loads are taken into account.

Table 1. Basic load states - engineering (Eng) and control theory (CT) notation

Load status	Load type	Notation (Eng)	Notation (CT)
0	Girder dead weight	$u_0, w_0, \alpha_0, M_0, Q_0, N_0$	$y_i, i = 1, \dots, 6$
1	Sheathing weight	$u_1, w_1, \alpha_1, M_1, Q_1, N_1$	$y_i, i = 7, \dots, 12$
2	Wind from the left – option I	$u_2, w_2, \alpha_2, M_2, Q_2, N_2$	$y_i, i = 13, \dots, 18$
3	Wind from the left – option II	$u_3, w_3, \alpha_3, M_3, Q_3, N_3$	$y_i, i = 19, \dots, 24$
4	Wind from the right – option I	$u_4, w_4, \alpha_4, M_4, Q_4, N_4$	$y_i, i = 25, \dots, 30$
5	Wind from the right – option II	$u_5, w_5, \alpha_5, M_5, Q_5, N_5$	$y_i, i = 31, \dots, 36$
6	Snow- option I	$u_6, w_6, \alpha_6, M_6, Q_6, N_6$	$y_i, i = 37, \dots, 42$
7	Snow from the left - option II	$u_7, w_7, \alpha_7, M_7, Q_7, N_7$	$y_i, i = 43, \dots, 48$
8	Snow from the right – option II	$u_8, w_8, \alpha_8, M_8, Q_8, N_8$	$y_i, i = 49, \dots, 54$

Jumps in the intensity of a distributed load can be accounted for using indicator functions [12] without adding characteristic points to the mathematical model. Therefore, the concentrated forces are replaced by equivalent distributed loads. The symmetry of the structure must lead to a symmetric solution. Since the analyzed girder axis is symmetrical, every basic nonsymmetric load is complemented by its mirror image (see Table 1).

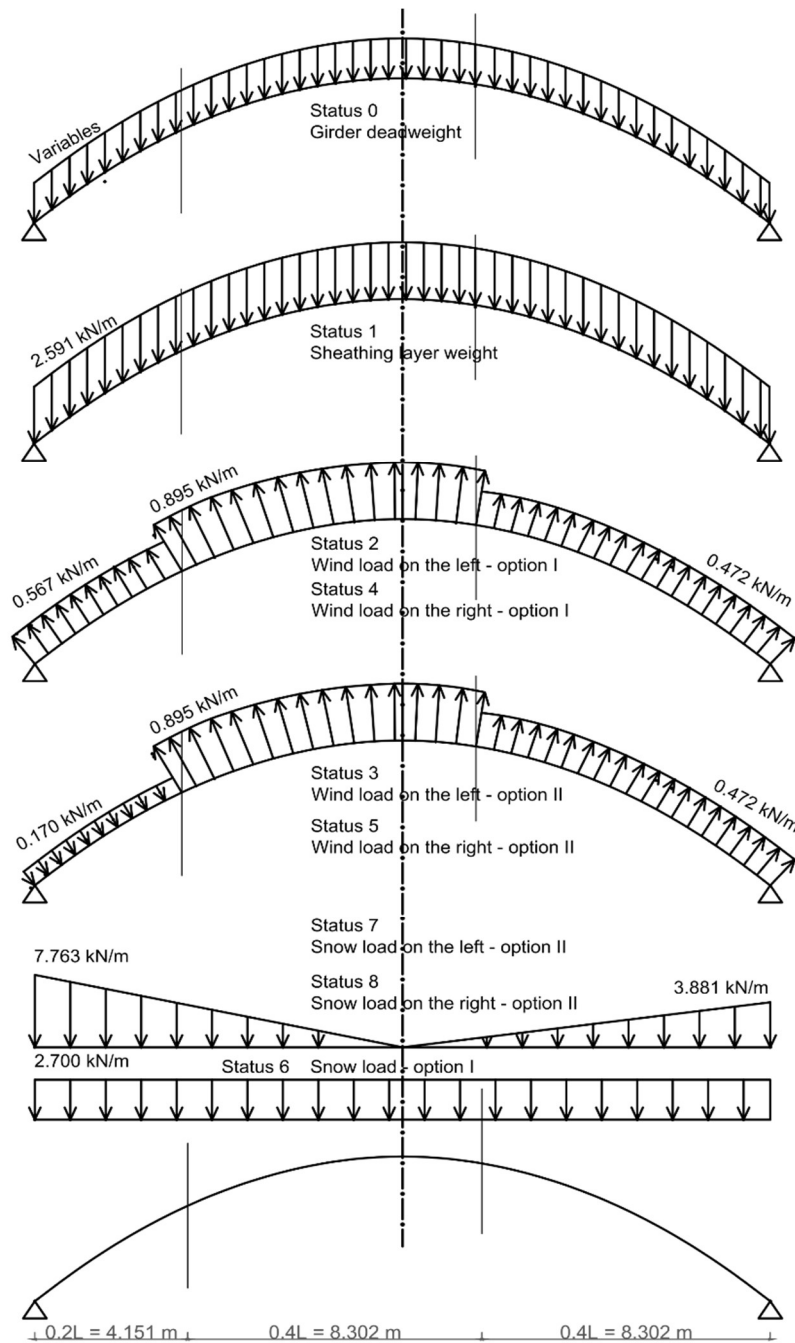


Fig. 2. Basic distributed load states

Table 2. Load configurations

Load configuration	Basic load status								
	0	1	2	3	4	5	6	7	8
1	+	+	+						
2	+	+		+					
3	+	+			+				
4	+	+				+			
5	+	+					+		
6	+	+						+	
7	+	+							+
8	+	+	+				+		
9	+	+	+					+	
10	+	+	+						+
11	+	+		+			+		
12	+	+		+				+	
13	+	+		+					+
14	+	+			+		+		
15	+	+			+			+	
16	+	+			+				+
17	+	+				+	+		
18	+	+				+		+	
19	+	+				+			+

The same rule holds when defining load combinations. The basic load states collated in Table 1 allow for the formation of 19 load combinations: 7 combinations of dead loads and a single environmental load (wind or snow) and 12 combinations of dead loads and two environmental loads (wind and snow) (see Table 2). The combination including only dead weights (load statuses 0 and 1) is ignored due to its minor importance. Basic load states are implemented in the state equations, whereas load combinations are defined during constraint formulation.

2.2. State equations in basic load states

In each of the 9 basic load stages, a set of 6 equations describes the parabolic arch under the action of consecutive load states

$$\begin{aligned}
 \frac{du_j}{dx} &= \left(\frac{N_j}{EA} + w_j \kappa \right) \cdot \frac{1}{\cos(\phi)}, & \frac{dw_j}{dx} &= \frac{-u_j \kappa + \alpha_j}{\cos(\phi)}, \\
 \frac{d\alpha_j}{dx} &= \frac{M_j}{EJ \cos(\phi)}, & \frac{dM_j}{dx} &= \frac{Q_j}{\cos(\phi)}, \\
 \frac{dQ_j}{dx} &= \frac{N_j \cdot \kappa - p_j}{\cos(\phi)}, & \frac{dN_j}{dx} &= \frac{Q_j \cdot \kappa - n_j}{\cos(\phi)}, \quad j = 0, 1, \dots, 8
 \end{aligned} \tag{2.1}$$

where:

u, w - displacements tangent and normal to the arc axis, M - bending moment, Q, N - shearing and axial forces, x - independent variable (see Fig. 1a), E - Young's modulus, A - cross-sectional area, J - moment of inertia, κ - axis curvature, ϕ - the inclination angle of the girder axis towards the x axis, α - rotation angle, p, n - load components tangent and normal to the axis. It should be noted that the cross-sectional area of the girder, the inertia moment, and load components of the zeroth load state p_0, n_0 depend on unknown cross-sectional dimensions $U_1(x)$ and $U_2(x)$.

The girder, in all load states, is described by 54 state equations. In addition, the equation for the arch mass ($W = y_{55}$) must be formulated

$$\frac{dW}{dx} = \frac{\gamma}{g} \cdot \frac{A}{\cos \phi}, \quad W(0) = 0 \tag{2.2}$$

where γ is the steel specific weight, g - gravitational acceleration. The state equations (2.1) and (2.2) are complemented by the boundary conditions, depending on the arch supports:

$$\begin{aligned}
 u_j(0) = 0, \quad w_j(0) = 0, \quad M_j(0) = 0, \quad W(0) = 0, \\
 u_j(l) = 0, \quad w_j(l) = 0, \quad M_j(l) = 0, \quad j = 0, 1, \dots, 8.
 \end{aligned} \tag{2.3}$$

The state equations are expressed as differential equations of the first order with proper boundary conditions. This approach allows for the formulation of the cross-section optimal shaping task within the framework of control theory with application of the maximum principle.

In classical control theory problems, time is the independent variable and the analyzed system is in motion. In statics issues, the concept of time loses its meaning, but by analogy one can take the x -coordinate of the bar axis as the

independent variable. This approach allows for utilizing the optimal control theory in structural mechanics problems.

2.3. Constraints

Based on the appropriate standard [3], the following constraints are imposed on the solution:

- limit of the normal stress on the bottom surface of the girder σ_{fd}

$$G_1 = f_d - \sigma_{fd} \quad (2.4)$$

- limit of the normal stress on the top surface of the girder σ_{fg}

$$G_2 = f_d - \sigma_{fg} \quad (2.5)$$

- limit of the complex stress state on the edge of the web σ_{fw}

$$G_3 = 1.1f_d - \sigma_{fw} \quad (2.6)$$

- limit of the shear stress on the girder axis τ_f

$$G_4 = 0.58f_d - \tau_f \quad (2.7)$$

- limit of the maximal deflection z

$$G_5 = c - z \quad (2.8)$$

where:

f_d - steel design strength, c - allowable deflection.

The stresses appearing in Eqs. (2.4)-(2.7) are determined as the extreme values that can occur under any of the 19 analyzed load combinations, which can be formulated by means of the maximum function. For example, in formula (2.4)

$$\sigma_{fd} = \max \{ |\sigma_{fd,i}| \}, \quad i = 1, 2, \dots, 19. \quad (2.9)$$

Load combinations are defined during the formulation of constraint functions. According to Table 2, in Eq.(2.9), the elements of the set $\{ |\sigma_{fd,i}| \}$ take the form

$$\begin{aligned} \sigma_{fd,1} &= |\sigma_{0d} + \sigma_{1d} + \sigma_{2d}| \\ \sigma_{fd,2} &= |\sigma_{0d} + \sigma_{1d} + \sigma_{3d}| \\ &\dots \\ \sigma_{fd,19} &= |\sigma_{0d} + \sigma_{1d} + \sigma_{5d} + \sigma_{8d}| \end{aligned} \quad (2.10)$$

where: σ_{jd} means the normal stress on the bottom surface in the j^{th} basic state.

The deflection z in constraint (2.8) is defined as

$$z = \max(Z_1, Z_2, \dots, Z_{19}), \quad (2.11)$$

where, in accordance with load combinations

$$\begin{aligned} Z_1 &= |u_0 \sin \phi + w_0 \cos \phi + u_1 \sin \phi + w_1 \cos \phi + u_2 \sin \phi + w_2 \cos \phi| \\ Z_2 &= |u_0 \sin \phi + w_0 \cos \phi + u_1 \sin \phi + w_1 \cos \phi + u_3 \sin \phi + w_3 \cos \phi| \end{aligned} \quad (2.12)$$

....

$$Z_{19} = |u_0 \sin \phi + w_0 \cos \phi + u_1 \sin \phi + w_1 \cos \phi + u_5 \sin \phi + w_5 \cos \phi + u_8 \sin \phi + w_8 \cos \phi|.$$

Such a notation allows for a significant reduction of the number of constraints in the analyzed optimization problem. Additional constraints define upper and lower bounds imposed on the decision variables by design, technological, and manufacturing requirements

$$U_k \in U_{admissible} : U_1 \in \langle 0.05, 0.16 \rangle, U_2 \in \langle 0.005, 0.008 \rangle. \quad (2.13)$$

3. FORMULATION OF THE OPTIMIZATION TASK

Within the framework of the maximum principle, the objective is to determine two unknown cross-sectional dimensions $U_1(x)$ and $U_2(x)$ of the arch girder described by the set of equations (2.1), which provide the minimum mass, expressed as

$$W(U_1, U_2) = \frac{\gamma}{g} \int_0^l \frac{A}{\cos \phi} dx \quad (3.1)$$

under the condition that both the load carrying capacity and displacement limits are not exceeded under any load combination

$$\min_{U_k} (W(l)). \quad (3.2)$$

This method allows for finding the solution that is optimal in mathematical terms and can be implemented in engineering practice. The inclusion of limits (2.13) imposes the physical meaning of the sought solution, excluding both zero and infinite cross-sections.

3.1. Solution method – optimization formalism

The engineering content of the presented optimization task leads to the optimal control problem of the Mayer type. One must determine controllers U_1 and U_2 that solve the following task:

$$\min_{U_1, U_2} (y_{55}(l)), \quad \frac{dy_{55}}{dx} = \frac{\gamma}{g} \cdot \frac{A}{\cos \phi}, \quad y_{55}(0) = 0,$$

$$\frac{dy_i}{dx} = f_i(x, y_i, U_k), \quad i = 1, 2, \dots, n_y = 54, \quad k = 1, \dots, n_u = 2, \quad f: R \times R^{n_y} \times R^{n_u} \rightarrow R^{n_y}, \quad (3.3)$$

$$G_s(y_i, U_k) \geq 0, \quad s = 1, \dots, n_g, \quad G_s: R^{n_y} \times R^{n_u} \rightarrow R, \quad n_g = 4$$

$$G_p(y_i) \geq 0, \quad p = 1, \dots, n_p, \quad G_p: R^{n_y} \rightarrow R, \quad n_p = 1$$

$y_r(0) = y_r(l) = 0$ for

$r = 1, 2, 4, 7, 8, 10, 13, 14, 16, 19, 20, 22, 25, 26, 28, 31, 32, 34, 37, 38, 40, 43, 44, 46, 49, 50, 52$

with the state functions $y_i: [0, l] \rightarrow R^{n_y}$ and the controls $U_k: [0, l] \rightarrow R^{n_u}$,

where: n_y - number of state variables, n_u - number of control variables, f_i - right hand sides of differential equations, n_g - number of control-state inequality constraints, n_p - number of pure-state inequality constraints.

The engineering task discussed in this paper leads to an optimal control problem with mixed control-state inequality constraints $G_s(y_i, U_k) \geq 0$ and a pure state inequality constraint $G_p(y_i) \geq 0$. Pure-state constraints are generally more difficult to deal with than mixed control-state constraints, since they do not explicitly depend on control U_k and y_i can be controlled only indirectly via propagation through the state equations. The important feature of the above formulated differential-algebraic optimization problem is the fact that the decision variables are present not only in the differential part of the operator (2.1) but also in the algebraic part (right-hand sides), leading to a non-autonomous problem.

It should be noted that the characteristic feature of structural mechanics tasks is the fact that conditions of initial ($y_i(x=0)$) and final ($y_i(x=l)$) states are specified only in part, for some state variables, contrary to most other mechanics optimization issues defined as two-point boundary value problems, where the initial ($\Theta(t=0)$) and final ($\Theta(t=t_1)$) states are fully known.

3.2. Necessary optimality conditions for non-autonomous problems

Let y_i, f_i, G_s be sectionally differentiable functions of their arguments and U_k be the optimal solution of system (3.3). Then there exist a vector function of adjoint variables $\lambda = (\lambda_1, \dots, \lambda_{n_y})$, and multipliers $\mu = (\mu_1, \dots, \mu_{n_g})$, such, that for the Hamiltonian

$$H = \sum_{i=1}^{55} \lambda_i \cdot f_i + \sum_{s=1}^4 \mu_s \cdot G_s \quad (3.4)$$

the following relations hold

$$\frac{d\lambda_i}{dx} = -\frac{\partial H}{\partial y_i}, \quad \frac{dy_i}{dx} = \frac{\partial H}{\partial \lambda_i}. \quad (3.5)$$

The complete proof of the transversal conditions (3.5) can be found in [5] and [21]. The adjoint variables corresponding to these state variables for which no boundary conditions were imposed must fulfill the following relations

$$\lambda_p(0) = \lambda_p(l) = 0 \quad (3.6)$$

for $p = 3, 5, 6, 9, 11, 12, 15, 17, 18, 21, 23, 24, 27, 29, 30, 33, 35, 36, 39, 41, 42, 51, 53, 54$.

If f_i and H are nonlinear functions, the Hamiltonian is regular, and the pure state constraints are not active ($G_p > 0$), then the following relation holds

$$\frac{\partial H}{\partial U_k} = \sum_{i=1}^{55} \lambda_i \cdot \frac{\partial f_i}{\partial U_k} + \sum_{s=1}^4 \mu_s \cdot \frac{\partial G_s}{\partial U_k} = 0 \quad k = 1, 2. \quad (3.7)$$

Formula (3.7) allows for the determination of Lagrange multipliers μ_s that meet the following condition

$$\mu_s(x) \begin{cases} = 0 & \text{if } G_s > 0 \\ > 0 & \text{if } G_s = 0. \end{cases} \quad (3.8)$$

In this case, the optimal control is calculated from the equation

$$G_s(y_i, U_k) = 0 \quad \text{for } x \in (x_1, x_2). \quad (3.9)$$

It should be noted that mixed state-control inequality constraints in structural mechanics problems are active mostly sectionally.

On the other hand, pure state inequality constraints are in most cases active only pointwise $G_p(x_c, y_i(x_c)) = 0$, where x_c are called contact points. These extra constraints give rise to jump conditions for the adjoint variables and the Hamiltonian function as

$$\begin{aligned} \lambda_w(x_c^-) &= \lambda_w(x_c^+) + \pi_{w_1} \frac{\partial G_5}{\partial y_w} \\ H(x_c^-) &= H(x_c^+) - \pi_{w_2} \frac{\partial G_5}{\partial x} \end{aligned} \quad (3.10)$$

for adjoint variables λ_w corresponding to appropriate state variables. In the engineering problem discussed in this paper, the pure state constraint limits the

arch deflection, so jumps can appear in λ_w corresponding to normal and tangent displacements.

In formula (3.10) $\pi_{w_1}, \pi_{w_2} \in R$ are Lagrange multipliers. The adjoint variables can be interpreted as the measure of sensitivity of the objective function to the change of the corresponding state variables. The necessary conditions (3.4)-(3.9) result in the boundary value problem with interior point constraints, i.e., a multipoint boundary value problem.

4. RESULTS AND DISCUSSION

Application of the formalism of the maximum principle presented in Sections 3.1 and 3.2 to the shape optimization problem of the steel arch leads to the multipoint boundary value problem built of 110 differential equations (55 state equations and 55 conjugated equations), 2 conditions for the minimum of the Hamilton function, 5 constrain functions, and 2 conditions for permissible controls. The problem dimensions are 55x55 for 110 ordinary differential equations. Since constructing a suitable starting approximation for the multi-shooting problem may be difficult, it is calculated using the direct collocation method software (Dircol). This method solves a parametrized version of the optimization task leading to stable values of adjoint variables. Through the application of the Dircol-2.1 software [29] two non-determined girder cross-sectional dimensions $U_1(x)$ and $U_2(x)$ are defined for which the objective function reaches the minimal value and the limitation state is not exceeded in any analytical scenario. The key role in this formulation is played by the structure of the control. In the analyzed problem, the control structure depends essentially on constraint $y_d = c$ assumed in equation (2.8).

Adopting the allowable deflection $c = 0.07$ m, which corresponds to $\frac{1}{296.5}$ of the arch span l leads to the quality indicator $W = 605.31$ kg and the following control (Fig. 3)

$$U_1(x) = \begin{cases} 0.05 & x \in (0.0, 0.472) \\ U_{opt} & x \in (0.472, 1.415) \\ 0.16 & x \in (1.415, 19.811) \\ U_{opt} & x \in (19.811, 20.282) \\ 0.05 & x \in (20.282, 20.754) \end{cases} \quad G_5 = 0 \text{ for } x_1 = 4.245 \text{ and } x_2 = 16.509 \quad (3.11)$$

$$U_2(x) = \begin{cases} 0.005 & x \in (0.0, 1.887) \\ U_{opt} & x \in (1.887, 2.830) \\ 0.008 & x \in (2.830, 6.132) \\ U_{opt} & x \in (6.132, 7.075) \\ 0.005 & x \in (7.075, 13.679) \\ U_{opt} & x \in (13.679, 14.622) \\ 0.008 & x \in (14.622, 17.924) \\ U_{opt} & x \in (17.924, 18.867) \\ 0.005 & x \in (18.867, 20.754) \end{cases} \quad G_5 = 0 \text{ for } x_1 = 4.245 \quad G_5 = 0 \text{ for } x_2 = 16.509 \quad (3.12)$$

Adoption of $c = 0.075 \text{ m}$ changes the control structure, U_1 takes the form (3.13) (see Fig. 3) whereas $U_2 = 0.005$ for every $x \in (0, l)$. The quality indicator is reduced to $W = 527.39 \text{ kg}$

$$U_1(x) = \begin{cases} 0.05 & x \in (0.0, 0.847) \\ U_{opt} & x \in (0.847, 2.118) \\ 0.16 & x \in (2.118, 7.200) \\ U_{opt} & x \in (7.200, 13.554) \\ 0.16 & x \in (13.554, 18.636) \\ U_{opt} & x \in (18.636, 19.907) \\ 0.05 & x \in (19.907, 20.754). \end{cases} \quad G_5 = 0 \text{ for } x_1 = 4.245 \quad G_5 = 0 \text{ for } x_2 = 16.518 \quad (3.13)$$

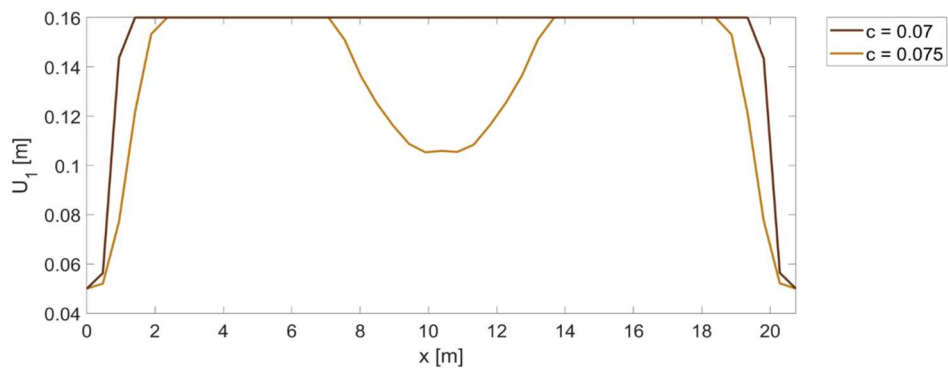


Fig. 3. Optimal solution U_1 with the active constraint $G_5 = 0$.

Further increasing the allowable deflection leads to subsequent changes in the control structure, resulting in the activation of stress constraint $G_2 = 0$ (see

Equation (2.5)). For c ranging from 0.08 to 0.12 m two constraints G_2 and G_5 are active simultaneously (see Fig. 4). For $c = 0.09 m$ this structure takes the form

$$U_1(x) = \begin{cases} 0.05 & x \in (0.0, 0.847) \\ U_{opt} & x \in (0.847, 3.388) & G_2 = 0 \text{ for } x \in (0.847, 1.694) \\ 0.16 & x \in (3.388, 5.506) & G_5 = 0 \text{ for } x_1 = 4.236 \\ U_{opt} & x \in (5.506, 9.318) \\ 0.05 & x \in (9.318, 11.436) \\ U_{opt} & x \in (11.436, 15.671) \\ 0.16 & x \in (15.671, 17.789) & G_5 = 0 \text{ for } x_2 = 16.518 \\ U_{opt} & x \in (17.789, 19.907) & G_2 = 0 \text{ for } x \in (19.060, 19.907) \\ 0.05 & x \in (19.907, 20.754) \end{cases} \quad (3.14)$$

with accompanied arch mass $W = 438.37 \text{ kg}$.

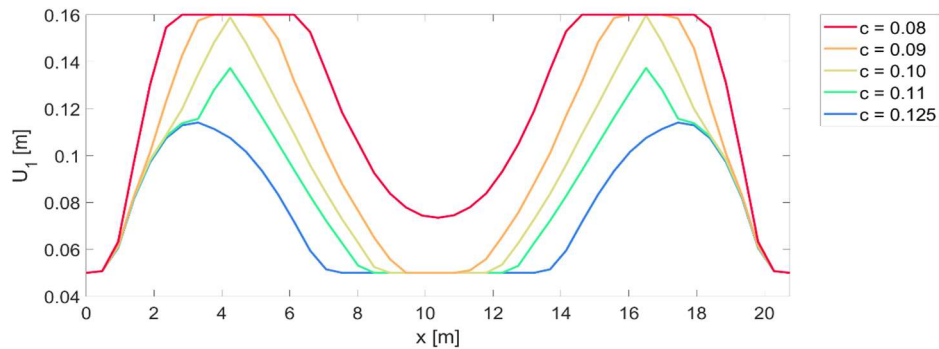


Fig. 4. Optimal solutions U_1 with active constraints $G_2 = 0$ as well as $G_5 = 0$.

For $c = 0.125 m$ the constraint G_5 is no longer active, resulting in the steady control structure (see Fig. 5 and Table 3) given by the formula

$$U_1(x) = \begin{cases} 0.05 & x \in (0, 0.847) \\ U_{opt} & x \in (0.847, 6.777) & G_2 = 0 \text{ for } x \in (0.847, 8.353) \\ 0.05 & x \in (6.777, 13.977) \\ U_{opt} & x \in (13.977, 19.907) & G_2 = 0 \text{ for } x \in (13.977, 19.907) \\ 0.05 & x \in (19.907, 20.754). \end{cases} \quad (3.15)$$

The mass of the optimal arc in this case is reduced to $W = 353.66 \text{ kg}$.

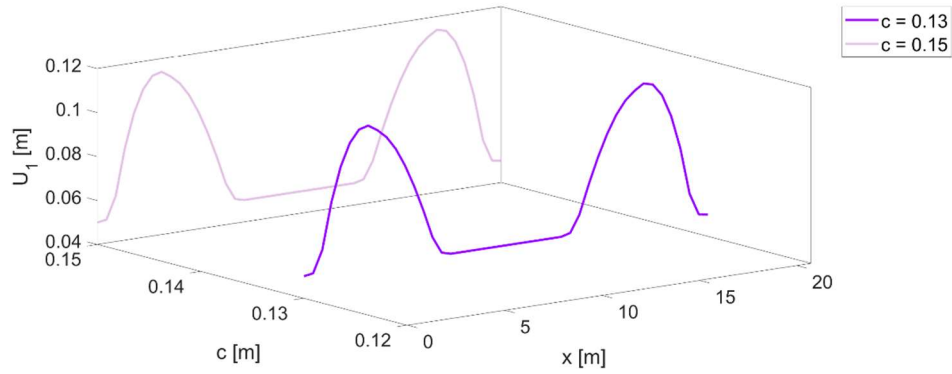


Fig. 5. Optimal solutions U_1 with the active constraint $G_2 = 0$.

The comparison of the optimal solution U_1 in all discussed cases is presented in Fig. 6.

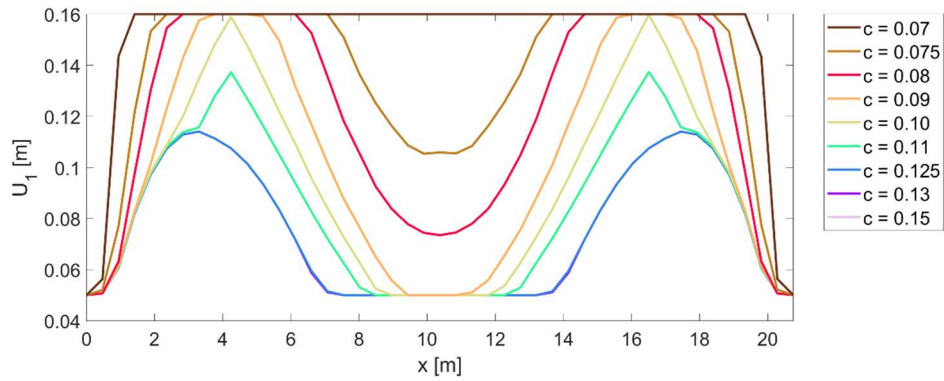
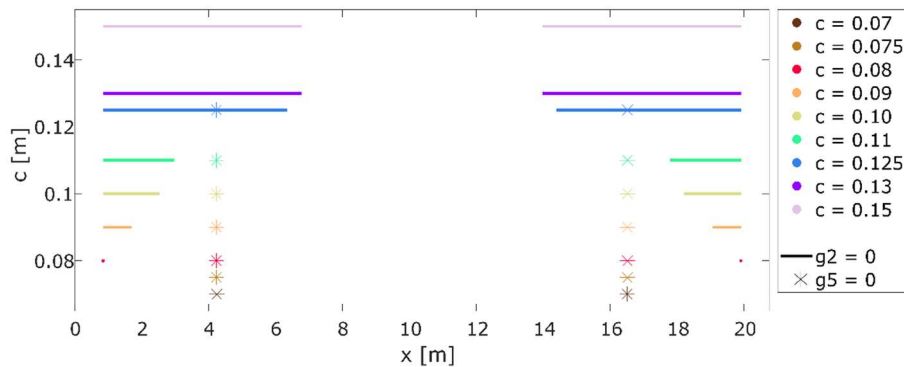


Fig. 6. Summary of optimal solutions U_1 for different values of c

Table 3 and Fig. 7 show the ranges of activity of the constraints and values of the corresponding quality indicators.

Table 3. Optimization results for different permissible deflections c .

$c[m]$	$W[kg]$	$G_2 = 0$	$G_5 = 0$
0.07	605.31	-	$x_1 = 4.245, x_2 = 16.509$
0.075	527.39	-	$x_1 = 4.236, x_2 = 16.518$
0.08	488.33	$x_1 = 0.847, x_2 = 19.907$	$x_1 = 4.236, x_2 = 16.518$
0.09	438.37	$x \in (0.847 - 1.694), (19.060, 19.907)$	$x_1 = 4.236, x_2 = 16.518$
0.096	417.49	$x \in (0.847 - 2.118), (18.636, 19.907)$	$x_1 = 4.236, x_2 = 16.518$
0.1	405.68	$x \in (0.847 - 2.541), (18.213, 19.907)$	$x_1 = 4.236, x_2 = 16.518$
0.11	381.03	$x \in (0.847 - 2.965), (17.789, 19.907)$	$x_1 = 4.236, x_2 = 16.518$
0.12	362.27	$x \in (0.847 - 3.812), (16.942, 19.907)$	$x_1 = 4.236, x_2 = 16.518$
0.125	354.79	$x \in (0.847 - 6.353), (14.401, 19.907)$	$x_1 = 4.236, x_2 = 16.518$
0.13	354.66	$x \in (0.847 - 6.777), (13.977, 19.907)$	-
0.15	354.66	$x \in (0.847 - 6.777), (13.977, 19.907)$	-

Fig. 7. Activeness of constraints $G_2 = 0$ and $G_5 = 0$ in terms of c

To verify the results of the optimization procedure, the FEM models of the arch with the above presented optimal cross-sections are built and analyzed in the Abaqus software, checking for both ultimate and serviceability limit states under the action of all 19 load combinations. The arch FEM model is constructed from 200 linear Euler-Bernoulli beam elements, to adjust the beam model to the conditions accounted for in the optimization problem. The stress and deflection envelopes (gathered from all load combinations) for the initial (constant) and chosen optimal cross-sections are presented in Figs 8 and 9. It can be seen that all constraints (2.4)-(2.8) imposed on stresses and deflections are satisfied for all optimal arches.

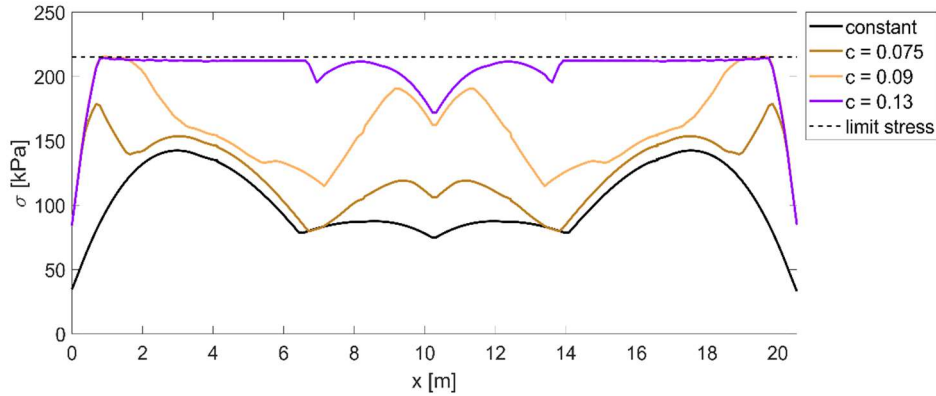


Fig. 8. Stress envelopes for arches with constant (initial) and optimal cross-sections

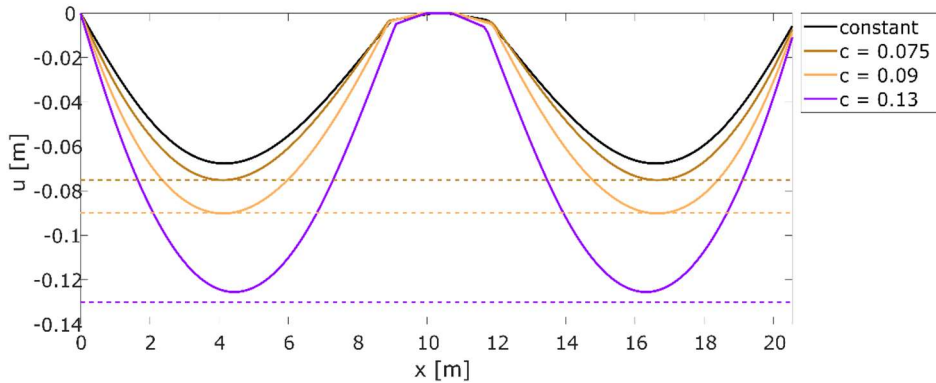


Fig. 9. Deflection envelopes for arches with constant (initial) and optimal cross-sections together with allowable deflections

4.1. Discussion

Optimal control problems with state inequality constraints frequently arise in practical applications. These problems are notoriously hard to solve and even the theory is ambiguous, since there exist various forms of necessary conditions of optimality.

The main benefit from the application of this indirect method is its high accuracy (obtained optimality tolerance equals 10^{-6} and nonlinear feasibility tolerance equals 10^{-5}), which is unattainable in direct methods.

Computations in Dircol 2.1 must be preceded by introducing initial values of the state variables, which are automatically corrected in subsequent iterations until the final solution, fulfilling the necessary optimality conditions, is determined. The activeness of the constrains is presented in Fig. 7. The obtained

results fulfill all the necessary optimality conditions, the boundary conditions, and the imposed constraints. The dependence of the quality indicator on the allowable deflection c is presented in Fig. 10. The benefits arising from the optimization process, measured by the reduction of the structure mass, amount to 42%.

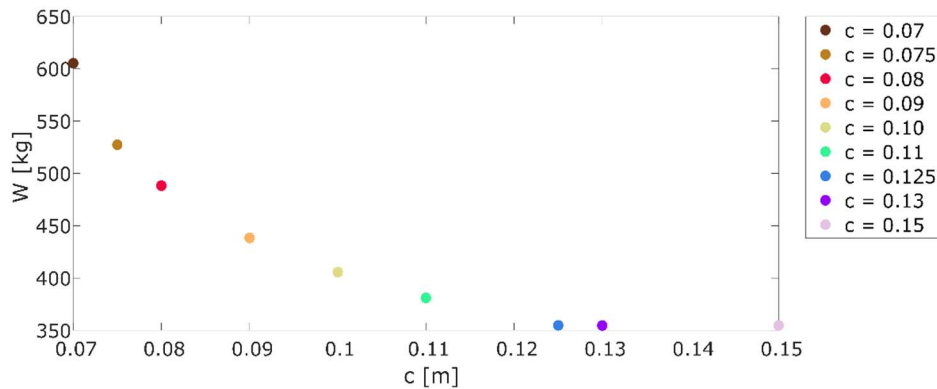


Fig. 10. Quality indicator in terms of c

Particularly important is the assumption of the proper control structure. Dircol software helps to define the control structure leading to a convergent solution of the multipoint boundary value problem, fulfilling all necessary optimality conditions.

Analysis of the course of variability of adjoint variables allows for identifying the least favorable load combinations that lead to constraint activation. Jumps in these graphs indicate points at which the deflection constraint is active. For instance for allowable deflection $c = 0.09\text{ m}$ two symmetrical load combinations 10 and 15 activate this serviceability limit state at points $x_1 = 4.236\text{ m}$ and $x_2 = 16.518\text{ m}$ accordingly. Figs. 11 and 12 show the displacements and the corresponding adjoint variables for the 7th and 8th basic load states. Analogical jumps appear in displacement-related adjoint variables for the 0th, 1st, and 2nd basic load states at point x_1 and for the 0th, 1st, and 4th basic load states at point x_2 , since these states build combinations 10 and 15 (see Table 2). Fig. 13 presents the objective function and the Hamiltonian for this permissible deflection value.

The optimal solution fulfils all the formal requirements and the necessary optimality conditions. However, it should be noted that there is no guarantee that the determined configuration constitutes the global minimum.

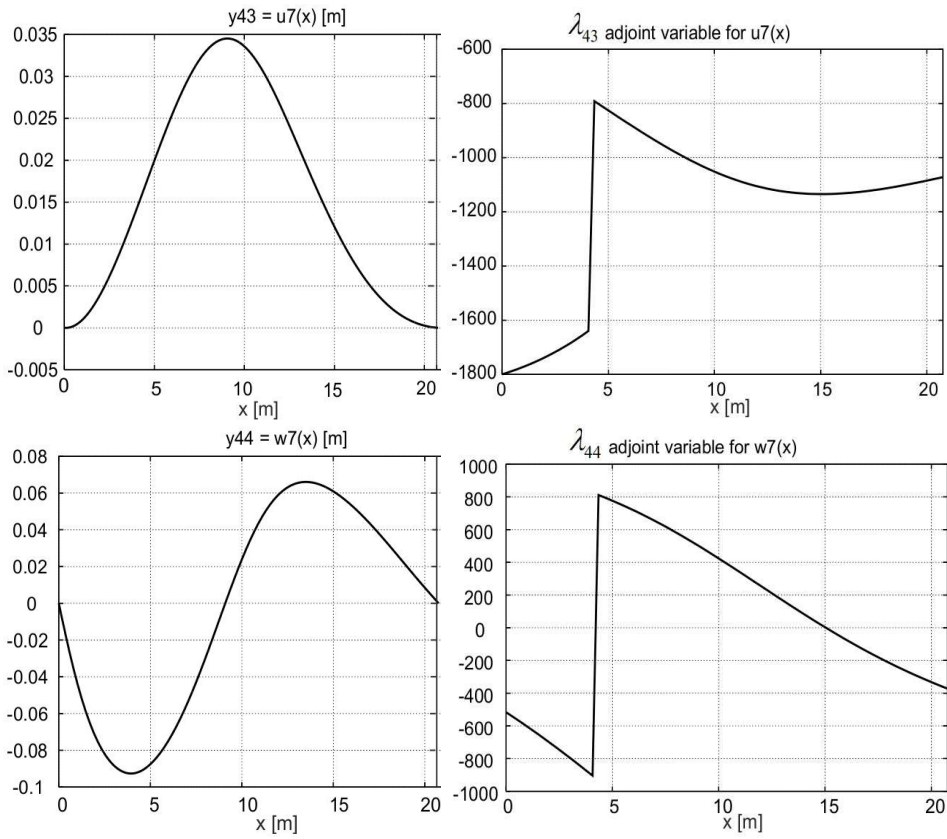


Fig. 11. State variables y_{43} , y_{44} (displacements under the 7th basic load) with corresponding adjoint variables for $c = 0.09$.

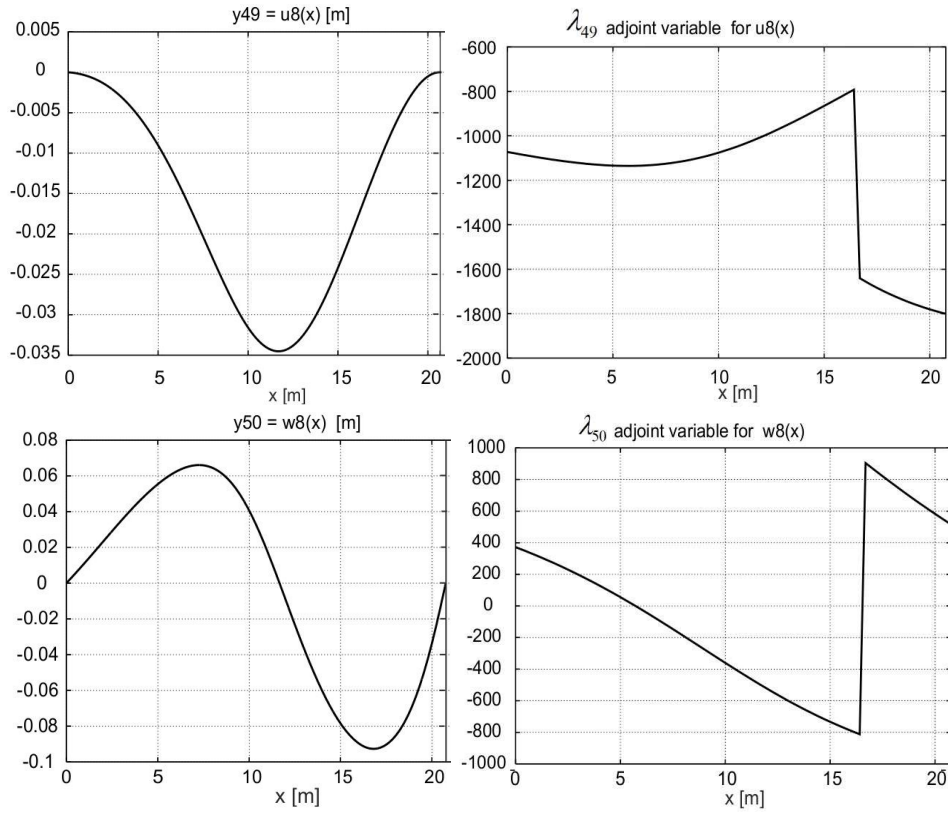


Fig. 12. State variables y_{49}, y_{50} (displacements under the 8th basic load) with corresponding adjoint variables for $c = 0.09$.

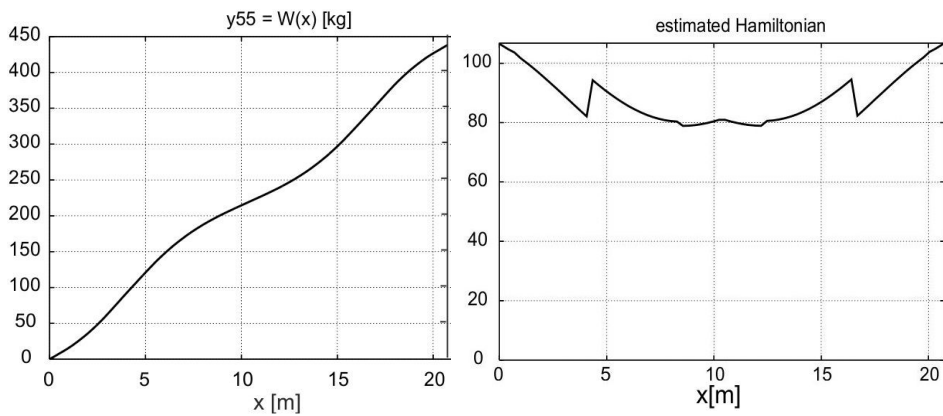


Fig. 13. The objective function and the Hamiltonian for $c = 0.09m$.

5. CONCLUSIONS

Calculations based on the maximum principle allowed for the determination of the cross-sectional dimensions of the arch steel girder whose mass proved to be much smaller than that resulting from conventional calculations (material savings amount up to 42 %). However, taking into account the relation of material savings to associated probable labor costs, it must be concluded that for such slender elements the material savings may not be significant enough.

The advantage of this method is that the optimal solution fulfilling the assumed ultimate and serviceability limit states can be determined for many load combinations in any analytical scenario.

Essential effects of this work:

- determination of the optimal control structure that ensures the convergence of the optimization process for this multi-decision and multi-constraint problem;
- using the maximum function while formulating constraints for multiple load states, significantly reducing their number;
- verification of the activity of constraints for optimal solutions by FEM calculations, which confirms that optimal arches fulfill the requirements imposed by design standards;
- numerical solution of a multipoint boundary value problem (MPBVP) of large dimensions (110 differential equations). The dimension of MBBVP is an indicator of the complexity of the problem;
- analysis of the impact of the permissible deflection constraint on the optimal solution structure.

The achieved solution confirms that optimal control theory can be successfully applied to optimal shaping of engineering structures. Such solutions can be employed in engineering practice or constitute a measure of design effectiveness.

ADDITIONAL INFORMATION

This research was supported in part by PLGrid Infrastructure.

REFERENCE

1. Allen, E and Zalewski, W 2009. *Form and Forces: Designing Efficient, Expressive Structures*. Hoboken:John Wiley & Sons, Incorporated.
2. Bessini, J, Shepherd, P, Monleón, S and Lázaro, C 2020. Design of bending-active tied arches by using a multi-objective optimization method. *Structures*. **27**. 2319–2328.

3. EN 1991-1-1: Eurocode 1: Actions on structures - Part 1-1: General actions - Densities, self-weight, imposed loads for buildings [Authority: The European Union Per Regulation 305/2011, Directive 98/34/EC, Directive 2004/18/EC].
4. Fiore, A, Marano, GC, Greco, R and Mastromarino, E 2016. Structural optimization of hollow-section steel trusses by differential evolution algorithm. *Int. J. Steel Struct* **16**(2). 411–423.
5. Hartl, RF, Sethi, SP and Vickson, RG 1995. A Survey of the Maximum Principles for Optimal Control Problems with State Constraints. *SIAM Rev.* **37** (2). 181–218.
6. Jasińska, D and Kropiowska, D 2018. The Optimal Design of an Arch Girder of Variable Curvature and Stiffness by Means of Control Theory. *Math. Probl. Eng.* **2018** p. 8239464.
7. Karamzin, D and Pereira, FL 2019. On a Few Questions Regarding the Study of State-Constrained Problems in Optimal Control. *J. Optim. Theory Appl.* **180** (1). 235-255.
8. Kimura, T, Ohsaki, M.; Fujita, S, Michiels, T and Adriaenssens, S 2020. Shape optimization of no-tension arches subjected to in-plane loading. *Structures*. **28**. 158–169.
9. Korytowski, A and Szymkat, M 2021. Necessary Optimality Conditions for a Class of Control Problems with State Constraint. *Games*. **12**(9), doi: 10.3390/g12010009.
10. Kropiowska, D and Mikulski, L 2009. Optimal design of two-hinged arches of the rational centre line. *Pomiary Autom. Kontrola*. **55**(6). 338–341.
11. Kropiowska, D, Mikulski, L and Styrna, M 2012. Optimal shaping of elastic arches in terms of stability. *Pomiary Autom. Kontrola* . **58**(10). 896–900.
12. Laskowski, H, Mikulski, L and Ostaficzuk, J 2007. Theoretical solutions and their practical applications in structure optimization. *Pomiary Autom. Kontrola*. **53**(8). 38–43.
13. Lewis, WJ 2016. Mathematical model of a moment-less arch. *Proceedings. Math. Phys. Eng. Sci.* **472**(2190). 20160019.
14. Mao, Y, Dueri, D, Szmuk, M and Açıkmeşe, B 2017. Successive Convexification of Non-Convex Optimal Control Problems with State Constraints. *IFAC-PapersOnLine*. **50**(1). 4063–4069.
15. Marano, G.C, Trentadue, F and Petrone, F 2014. Optimal arch shape solution under static vertical loads. *Acta Mech.* **225**(3). 679–686.
16. Marano, GC, Trentadue, F, Greco, R, Vanzi, I and Briseghella, B 2018. Volume/thrust optimal shape criteria for arches under static vertical loads. *J. Traffic Transp. Eng.* **5**(6). 503–509.
17. Mikulski, L 2004. Control Structure in Optimization Problems of Bar Systems. *Int. J. Appl. Math. Comput. Sci.* **14**(4). 515–529.

18. Mikulski, L 2007. *Theory of Control in Optimization of Structures and Systems (Teoria sterowania w problemach optymalizacji konstrukcji i systemów)*. Cracow. Cracow University of Technology Press.
19. Mikulski, L 2019. The Structure of the Optimal Control in the Problems of Strength Optimization of Steel Girders. *Arch. Civ. Eng.* **65**(4). 277–293.
20. Nodargi, NA and Bisegna, P 2020. Thrust line analysis revisited and applied to optimization of masonry arches. *Int. J. Mech. Sci.* **179**(2).105690.
21. Pesch, HJ 1996. A practical guide to the solution of real-life optimal control problems, *Control Cybern.* **23**(1).7–60.
22. Pesch, HJ and Plail, M 2009. The Maximum Principle of optimal control : A history of ingenious ideas and missed opportunities. *Control Cybern.* **38**(4). 973-995.
23. Pipinato, A 2018. Structural Optimization of Network Arch Bridges with Hollow Tubular Arches and Chords. *Mod. Appl. Sci.* **12**(2). 36-53.
24. Trentadue, F, Marano, G.C.; Vanzi, I and Briseghella, B 2018. Optimal arches shape for single-point-supported deck bridges. *Acta Mech.* **229**(5). 2291–2297.
25. Trentadue, F, Fiore, A, Greco, R, Marano, GC and Lagaros, ND 2020. Structural optimization of elastic circular arches and design criteria. *Procedia Manuf.* **44**. 425–432.
26. Trentadue, F et al. 2020. Volume optimization of end-clamped arches. *Hormigon y Acero.* **71**. 71–76.
27. Trentadue, F, Fiore, A, Greco, R, Marano, GC and Lagaros, ND 2020. Optimal Design of Elastic Circular Plane Arches. *Front. Built Environ.* **6**. art.74.
28. Vanderplaats, GN and Han, SH 1990. Arch shape optimization using force approximation methods. *Struct. Optim.* **2**(4). 193–201.
29. von Stryk, O 2002. *Users Guide. A Direct Collocation Method for the Numerical Solution of Optimal Control Problems*. Darmstadt. TU Darmstadt press.
30. Wang, CY and Wang, CM 2015. Closed-form solutions for funicular cables and arches. *Acta Mech.* **226**(5). 1641–1645.
31. Wilson, A 2005. *Practical Design of Concrete Shells*. Italy(TX). Monolithic Dome Institute.

Editor received the manuscript: 16.08.2022